Supplementary Data

Functional consequences of B-repeat sequence variation in the Staphylococcal biofilm protein Aap: Deciphering the assembly code

Catherine L. Shelton, Deborah G. Conrady, and Andrew B. Herr[1]

Program in Molecular Genetics, Biochemistry & Microbiology, University of Cincinnati College of Medicine, Cincinnati, OH 45267
Division of Immunobiology and Center for Systems Immunology, Cincinnati Children's Hospital Medical Center, Cincinnati, OH 45229
Division of Infectious Diseases, Cincinnati Children's Hospital Medical Center, Cincinnati, OH 45229

[1] Address correspondence to: Andrew B. Herr, Division of Immunobiology, Cincinnati Children's Hospital Medical Center, 3333 Burnet Ave., Cincinnati OH, 45229, USA.
Tel. 1-513-803-7490; Fax 1-513-636-5355; E-mail: andrew.herr@cchmc.org

Supplementary data files present in this document include:

1. **Supplementary Tables S1 and S2**
2. **Supplementary Figures S1 - S4**

Table S1. AUC sedimentation velocity parameters

Construct	s (Svedbergs)	f/f_0	MW (kDa)
8 μM $G5^{11}SpG5^{13}$	1.53[a]	1.96	25.3
8 μM $G5^{11}SpG5^{13*}$	1.53	1.94	24.3
8 μM $G5^{8}SpG5^{13}$	1.55	1.96	24.7
8 μM $G5^{8}SpG5^{13*}$	1.57	1.88	24.3
8 μM $G5^{11}SpG5^{13}$ + 5 mM $ZnCl_2$	2.20	1.46	27.9
8 μM $G5^{11}SpG5^{13*}$+ 5 mM $ZnCl_2$	1.59	1.84	24.7
8 μM $G5^{8}SpG5^{13}$ + 5 mM $ZnCl_2$	1.67	1.80	24.3
8 μM $G5^{8}SpG5^{13*}$ + 5 mM $ZnCl_2$	1.59	1.87	24.6
80 μM $G5^{11}SpG5^{13}$	1.53	1.96	25.2
80 μM $G5^{11}SpG5^{13*}$	1.53	1.96	25.6
80 μM $G5^{8}SpG5^{13}$	1.55	1.96	24.8
80 μM $G5^{8}SpG5^{13*}$	1.53	1.87	22.6
80 μM $G5^{11}SpG5^{13}$ + 5 mM $ZnCl_2$	2.68	1.63	44.4
80 μM $G5^{11}SpG5^{13*}$ + 5 mM $ZnCl_2$	1.68	1.77	25.2
80 μM $G5^{8}SpG5^{13}$ + 5 mM $ZnCl_2$	2.15	1.73	35.3
80 μM $G5^{8}SpG5^{13*}$ + 5 mM $ZnCl_2$	1.61	1.74	22.4

[a] *At the concentrations tested in this study (8 μM and 80 μM) the sedimentation coefficient of Brpt1.5 in the absence of zinc was between 1.53-1.57. This is consistent with the $s_{20,w}$ reported by Conrady et al of 1.55 for the monomeric $G5^{12}SpG5^{13}$ Brpt1.5 [20].*

Table S2. X-ray crystallography data collection and refinement statistics [a]

	$G5^{8}SpG5^{13}$ (VC)	$G5^{8}SpG5^{13*}$ (VV)	$G5^{11}SpG5^{13}$ (CC)
Data Collection			
Wavelength	0.984	0.979	1.033
Resolution range (Å)	42.4-1.90 (1.97-1.90) [b]	92.3-2.33 (2.41-2.33)	52.81-3.34 (3.46-3.34)
Space group	P 2_12_12	P 2_12_12	P 2_12_12
Unit cell dimensions (Å)	a, b, c, = 43.56, 54.95, 184.61	a, b, c = 43.62, 54.23, 184.498	a, b, c = 43.2, 55.1, 185.16
Observations	168,370	120,434	48,400
Unique reflections	35.511	19,223	6,919
Completeness (%)	99.0 (99.0)	98.0 (89.0)	100.0 (100.0)
Multiplicity	4.7 (4.7)	6.3 (4.6)	7.0 (7.1)
Mean I/sigma(I)	16.1 (2.77)	12.74 (2.52)	8.91 (2.67)
R_{merge}	0.068 (0.52)	0.153 (0.721)	0.230 (0.840)
R_{meas}	0.076 (0.59)	0.168 (0.814) Text	0.248 (0.906)
Refinement			
R_{work}/R_{free} (%)	21.7/23.9	21.0/24.4	25.6/30.7
Number of non-hydrogen atoms	2393	2234	1838
macromolecule	2040	2003	1827
Protein residues	276	271	259
rmsd bonds (Å)	0.007	0.013	0.003
rmsd angles (°)	0.77	1.84	0.57
Wilson B-factor	22.9	36.2	66.5
Average B-factor	36.4	50.7	52.3
macromolecule	36.8	51.4	52.4
solvent	34.1	45.3	37.4
Ramachandran favored (%)	100	100	98
Ramachandran outliers (%)	0	0	0
Rotamer outliers (%)	2.7	2.3	0
Clashscore [c]	3.77	3.33	4.63
Molprobity score/ percentile	1.43/97th	1.46/99th	1.24/100th

[a] Table was generated using phenix.table_one function in PHENIX
[b] Values in parenthesis refer to the highest resolution shell
[c] Structure validation was performed using the MolProbity server (http://molprobity.biochem.duke.edu/)

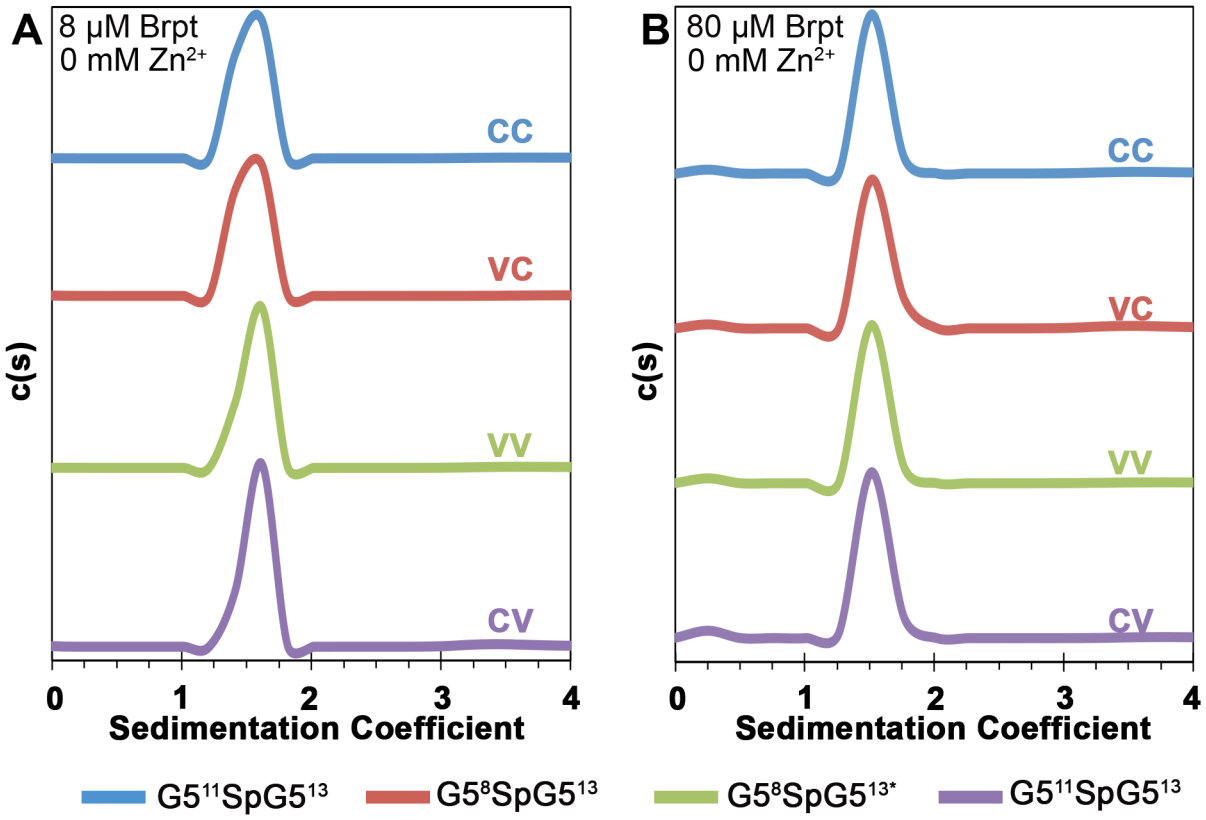

Figure S1
Sedimentation velocity analysis of monomeric Brpt1.5 constructs.
The sedimentation coefficient distribution for each construct is shown in the absence of Zn^{2+}, confirming that all constructs sediment as monomers as expected. Data were collected both at A) a lower concentration (8 μM) and B) 10-fold higher concentration (80 μM) to rule out Zn^{2+}-independent assembly events.

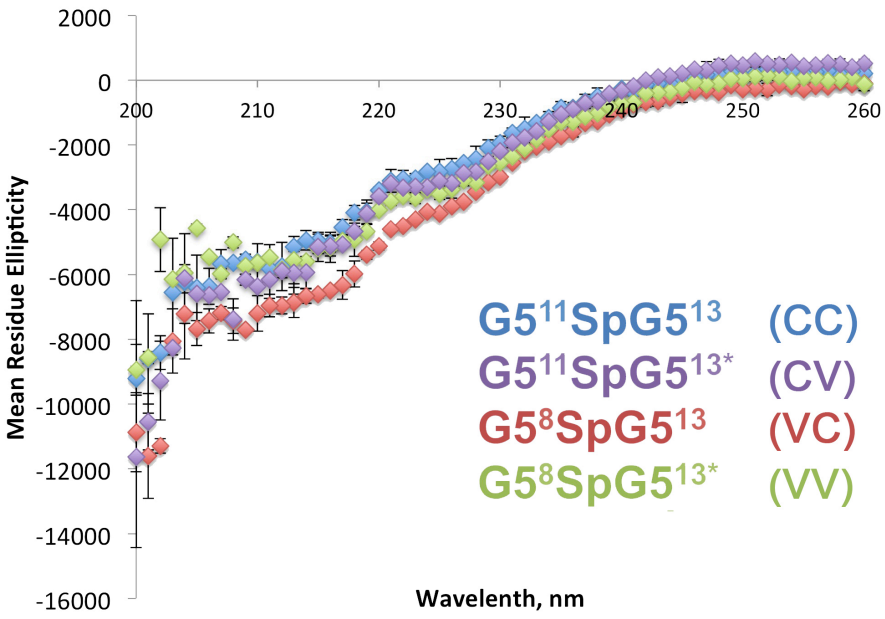

	G5[8]SpG5[13]	G5[8]SpG5[13*]	G5[11]SpG5[13]	G5[11]SpG5[13*]
α-helix	0.08	0.08	0.08	0.08
β-sheet	0.41	0.41	0.45	0.44
Random coil	0.51	0.51	0.48	0.48

Figure S2
Secondary structure content of Brpt1.5 constructs by far-UV circular dichroism.
After initial expression and purification, G5[11]SpG5[13] (CC), G5[11]SpG5[13*] (CV), G5[8]SpG5[13] (VC), and G5[8]SpG5[13*] (VV) were analyzed by circular dichroism between 200-260 nm to confirm that all constructs maintained similar overall folds. CD data deconvoluted using K2D indicates that all constructs are 40-45% β-sheet and 48-51% random coil.

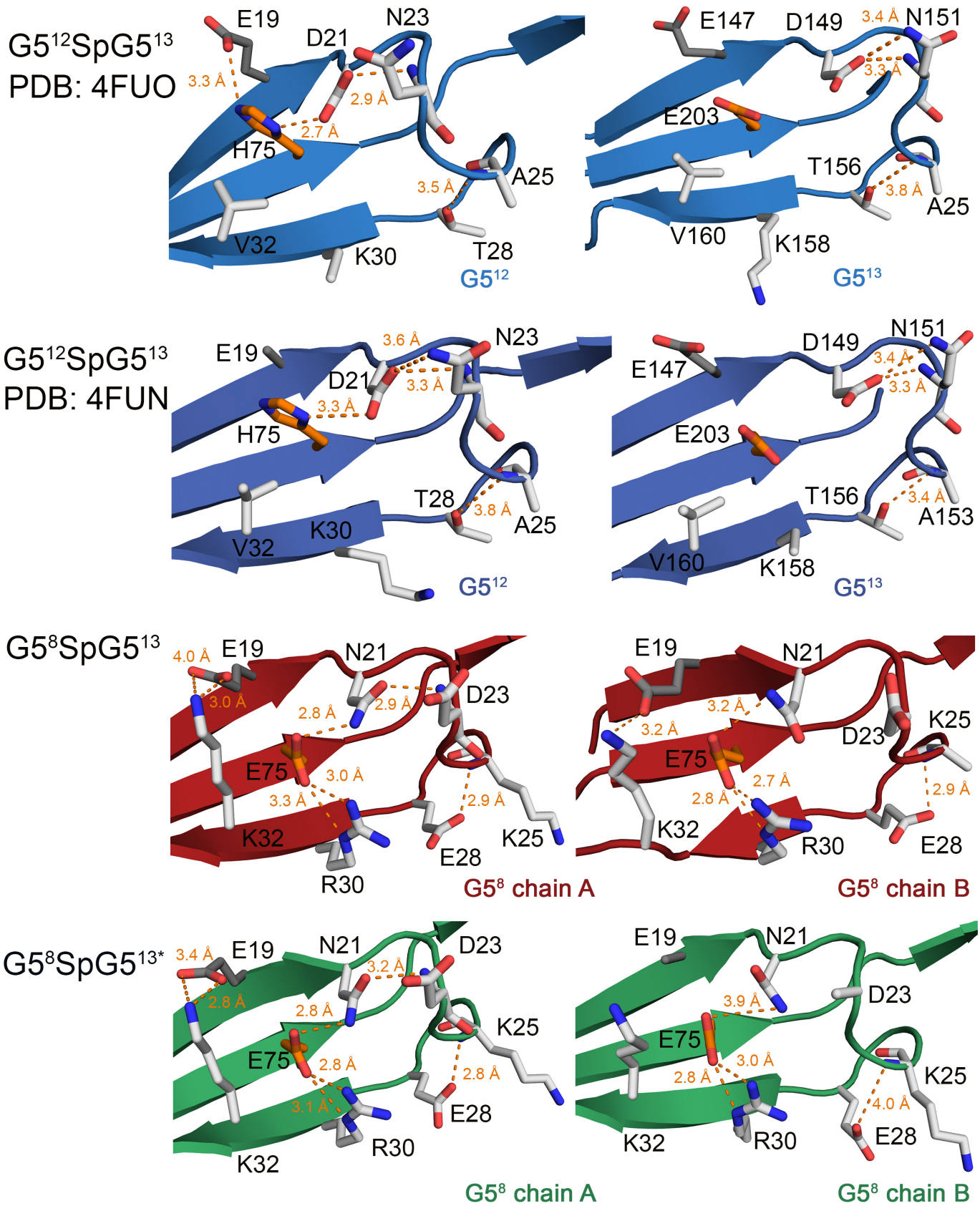
G5¹²SpG5¹³
PDB: 4FUO
E19
D21
N23
3.3 Å
2.9 Å
2.7 Å
H75
A25
3.5 Å
V32
K30
T28
G5¹²
E147
D149
3.4 Å
N151
3.3 Å
E203
T156
3.8 Å
A25
V160
K158
G5¹³
G5¹²SpG5¹³
PDB: 4FUN
E19
3.6 Å
N23
D21
3.3 Å
3.3 Å
H75
T28
3.8 Å
A25
V32
K30
G5¹²
E147
D149
N151
3.4 Å
3.3 Å
E203
T156
3.4 Å
A153
V160
K158
G5¹³
G5⁸SpG5¹³
4.0 Å
E19
N21
3.0 Å
2.8 Å
2.9 Å
D23
E75
3.0 Å
3.3 Å
2.9 Å
K32
K25
E28
R30
G5⁸ chain A
E19
N21
3.2 Å
3.2 Å
D23
K25
E75
2.7 Å
2.8 Å
2.9 Å
K32
R30
E28
G5⁸ chain B
G5⁸SpG5¹³*
3.4 Å
E19
N21
3.2 Å
D23
2.8 Å
2.8 Å
K25
E75
2.8 Å
2.8 Å
3.1 Å
E28
R30
K32
G5⁸ chain A
E19
N21
3.9 Å
D23
E75
3.0 Å
2.8 Å
K25
4.0 Å
K32
R30
E28
G5⁸ chain B

Figure S3

Consensus and variant G5 domains have different bonding networks.

Consensus G5 domains from the N- and C-terminus of two $G5^{12}SpG5^{13}$ crystal structures (PDB: 4FUO, 4FUN) are shown with blue or purple backbones. Residues that correspond to the variant cassette are shown in white sticks. Orange sticks indicate the variant amino acid that is a key zinc-binding residue (H/E75) to illustrate the approximate zinc-binding site. For the consensus G5, trans-strand bonding can only occur in the N-terminal G5 where H75 is within bonding distance of D21 and, in one case, E19. In the C-terminal G5 domains of the consensus constructs, no trans-strand bonding occurs and the only sidechain-to-sidechain bond occurs between D149 and N151. There are sidechain-to-backbone bonds between D149-N151 and T156-A153 which are not trans-strand, but occur in the same loop region. Those same sidechain-to-backbone bonds are also present in the N-terminal G5 of the consensus and variant constructs. Shown in red and green backbones are the variant G5 domains that were present in well-resolved density in the two monomers of each asymmetric unit of the new Brpt1.5 structures. Electron density for this region was uniformly better in chain A of both $G5^{8}SpG5^{13}$ (VC) and $G5^{8}SpG5^{13*}$ (VV) structures. In the N-terminal G5 domains from chain A of both variant constructs, the contact between E19-K32 and R30-E75 are particularly notable because of the potential for dual salt bridges between each set of residues. In chain B of $G5^{8}SpG5^{13}$ (VC, red), there is only a single bond between these two residues and in chain B of $G5^{8}SpG5^{13*}$ (VV, green) there is insufficient density to accurately position the E19 sidechain. Probable side chain orientations are shown for K25 and E28 in chain B of $G5^{8}SpG5^{13*}$ (VV, green) based on non-crystallographic symmetry, although these side chains are stubbed in the structure. In all four of the N-terminal variant G5 domains, E75—positioned in the central strand of the β-sheet—mediates a bonding network that spans the upper and lower strand of that sheet. It appears that the N21-D23 bonds that are present in the chain A variant G5 domains are absent in the chain B domains, which reduces the total number of bonds. Despite this reduction, the overall trend for increased bonds in the variant G5, especially trans-strand bonding networks, holds true for both variant structures.

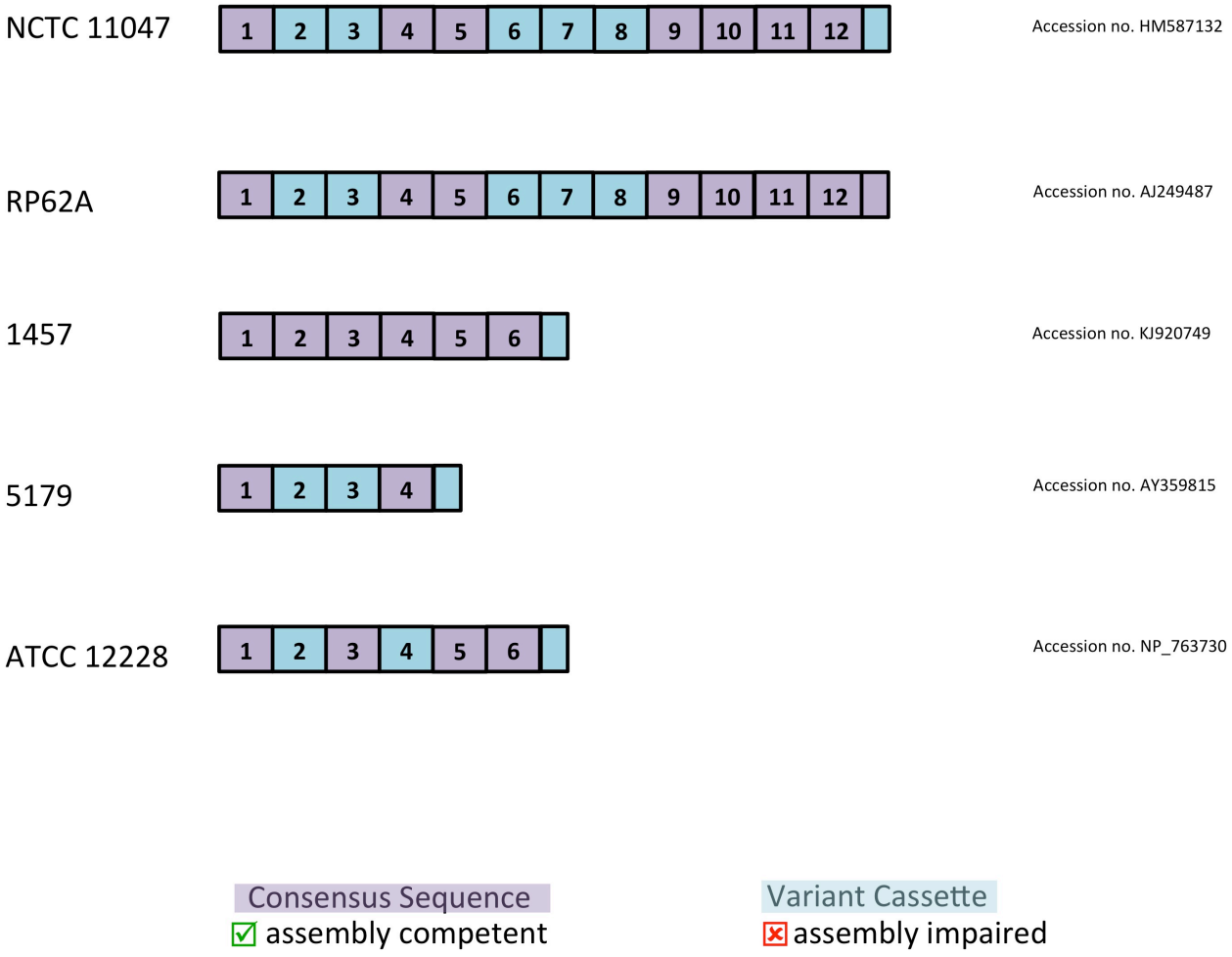

Figure S4
Aap B-repeat subtypes in multiple strains of *Staphylococcus epidermidis*.
The Aap sequences from *S. epidermidis* strains NCTC 11047, RP62A, 1457, 5179 and ATCC 12228 were analyzed for the presence of repeat subtypes in the B-repeat region. The distribution of repeat subtypes in these strains is shown as a cartoon with variant repeats shown in blue and consensus repeats shown in purple. Interestingly, each *S. epidermidis* strain shows the presence of B-repeat subtypes in Aap, although the specific distribution of consensus and variant repeats varies from strain to strain.